Joule

CellPress

Perspective

Challenges and Key Parameters of Lithium-Sulfur Batteries on Pouch Cell Level

Susanne Dörfler,[1] Holger Althues,[1] Paul Härtel,[1,2] Thomas Abendroth,[1] Benjamin Schumm,[1] and Stefan Kaskel[1,2,*]

Lithium-sulfur (Li-S) technology was identified as a promising candidate to overcome energy density limitations of common lithium-ion batteries given the world-wide abundance of sulfur as a low-cost alternative to state-of-the-art active materials, such as Ni and Co. Li-S cells have received tremendous recognition in recent years, both from a scientific and industrial perspective. However, only few data on adequate multilayer-pouch cell characterization are available so far, and transparent calculations on components require more consideration. Because of the gap of lab cell characterization and prototype cell development, misinterpretations and false expectations are frequently reported, mostly resulting from lithium and electrolyte excess. For the commercialization of the Li-S technology, rapid transfer of new concepts on the prototype cell level is essential. Furthermore, fundamental studies should concentrate on fundamental scientific questions related to the main bottlenecks of Li-S cells: understanding anode and electrolyte degradation phenomena and realistic evaluation of stabilizing interfaces.

PREMISES AND LIMITATIONS OF LITHIUM-SULFUR BATTERIES AS NEXT-GENERATION BATTERY SYSTEMS

Lithium-sulfur (Li-S) technology was identified as a promising candidate to overcome energy density limitations of common lithium-ion batteries as early as 1977[1–4] and has received tremendous recognition in recent years, both from a scientific and industrial perspective.[5–10] In the past decade, through fundamental scientific work on new material concepts, modeling, and analytical methods well over 1,000 peer-reviewed reports per year have been published. In addition, several prototype plants have been built and >460 Wh/kg[11–13] on the cell level has already been presented, indicating the principle feasibility of the cell concept. Especially, applications for which weight is a key parameter, in particular in aviation, profit from high specific energy cells. The most well-known applications are high altitude long endurance unmanned aerial vehicles (HALE UAVs). The best known of these systems are Project Loon, Facebook Aquila, and the Airbus Zephyr for geostationary high altitude pseudo-satellite (HAPS) navigation. Their solar battery charging during daytime and discharging at night requires only very low charging rates (approximately C/10) as one complete cycle takes 24 h. According to Fotouhi et al., future applications will depend on what improvements are made to Li-S, they break down into three areas: cycle life, power, and both cycle life and power. In addition, it is predicted that the heavy automotive vehicle market will be suitable, particularly for applications such as buses and trucks. Li-S cells would be useful here as the large batteries needed would be very heavy if Li-ion was used and Li-S could offer a weight

Context & Scale

Application-relevant data such as cycle life, rate capability, and energy density are inaccessible via electrochemical standard tests in today's Li-S-lab cells due to electrolyte and anode excess masking major degradation mechanisms. Because of the gap of lab cell characterization and prototype cell development, misinterpretations and false expectations of material development are frequently reported, and electrode porosity as well as pressure on cell stack are neglected.

Rapid transfer of new concepts on multilayer-pouch cell level is essential, especially for electrolytes working in lean electrolyte regime. Fundamental studies should concentrate on fundamental scientific questions related to the main bottlenecks of Li-S-cells: first, understanding anode and electrolyte degradation phenomena and realistic evaluation of stabilizing interfaces is crucial. Further, new analytical tools allowing electrochemical studies under lean electrolyte conditions and *in situ* studies of electrolyte and additive depletion pose tremendous chances for impactful

reduction. A 400 Wh/kg Li-S cell with good power capability (e.g., 5C+) but low cycle life will be useful to the following applications: smaller UAVs, such as hobby and/or short duration drones used for pleasure, mapping, deliveries, or photography would be able to fly longer and/or carry larger payloads.[14]

Furthermore, the world-wide abundance of sulfur is another important aspect for considering Li-S batteries as a sustainable and low-cost alternative to the nickel (Ni) and cobalt (Co) containing Li-ion batteries (LIB). Nevertheless, several main challenges are known impeding today's competitive commercialization of the Li-S battery. The cycling stability of Li-S prototype cells is usually limited because of Li-metal dendrite formation and electrolyte depletion. These degradation reactions at the anode surface are significantly affected by the highly complex conversion reactions.[5] In short, depending on the electrolyte system, soluble lithium polysulfides (LiPSs) emerge during the (dis-)charge process, diffuse to the anode as well as in un-filled volume of the cell out of the stack (dead volume) leading to active material loss, self-discharge, and other side effects. To overcome these limitations, promising new electrolytes, separators, carbon materials, and electrode designs have been introduced.[15] Promising concepts are, e.g., metallic lithium protection via lithium-conductive coatings,[16–18] carbon fiber-enhanced lithium films,[19] specially designed anions for solid electrolyte interface (SEI) stabilization,[20] and sparingly polysulfide solvating electrolytes.[21]

However, similar to lithium-metal versus oxide or rather nickel-manganese-cobalt oxides (NMC)-based batteries,[22] there is still a significant gap between scientific findings from lab-scale experiments and actual improvements on product level. This gap results from systematic deviations between few mAh lab (coin or Swagelok) cells and actual prototypes with capacities in the Ah range. Only little data on adequate multilayer-pouch cell characterization is available so far, although during the past decade, extensive academic research has been carried out, especially on cathode adaption.[23] In 2017, an intensive literature research within a perspective article on Li-S cells revealed that studies on practical cells need to be intensified as results obtained in bottom or coin cells are very often misleading, as discussed in detail in Cleaver et al.[15] Since 2017, an increasing number of articles published pouch cell results analyzing the translation from coin to pouch cell for lithium-metal batteries in general[24–27] and Li-S batteries in particular.[16,21,22,28–37] Nevertheless, values for Wh/kg on cell level, practical cathode areal capacities, low electrolyte amounts, and transparent calculations on components[13,16,28,30,35,36] are rarely found and require more consideration. Moreover, developments in regard of electrolyte formulations with low polysulfide solubility working under lean conditions have been made. Especially in electrolytes with high polysulfide solubility, the more sulfur that can be dissolved, the more sulfur will diffuse in different directions and precipitate. This might lead to inhomogeneous Li_2S and/or sulfur utilization during cycling and will negatively influence the cycling stability. Also, the more sulfur that is dissolved in the electrolyte, the more likely inhomogeneous reaction and hence SEI formation takes place. This also has a detrimental effect on the cycle stability. The electrolyte is hence a crucial key parameter in order to decrease polysulfide solubility and the accompanied issues that include active mass loss, low Coulombic efficiency, and the reaction of polysulfides with the metallic lithium anode. These findings also need rapid transfer to high energy prototype cells.[21,38]

While recent publications report on high cycle life (>1,000 cycles) and high specific capacities at high active material loadings in small lab cells,[15] actual prototype pouch cells still suffer from very fast degradation, mostly due to electrolyte depletion and anode degradation.[22,24]

research. In addition, tap density and the accompanied swelling and compaction behavior of cathodes in different electrolytes should be further addressed. Consequently, pressure distribution in pouch cells should be monitored and adapted to the respective mechanical properties of the cathode and anode. These guidelines help to realize a breakthrough of the Li-S technology as a sustainable, safe, and lightweight energy storage option in the near future.

[1]Fraunhofer Institute for Material and Beam Technology IWS, Winterbergstr. 28, 01277 Dresden, Germany

[2]TU Dresden, Department for Inorganic Chemistry 1, 01069 Dresden, Germany

*Correspondence: stefan.kaskel@chemie.tu-dresden.de

https://doi.org/10.1016/j.joule.2020.02.006

The reason behind will be thoroughly discussed later on, after comparing typical lab cells with prototype pouch cells. As a consequence of these unsolved issues, a wide commercialization of practically relevant Li-S cells has not been achieved so far, and the strong discrepancy between high level academic research but limited performance at prototype cell level is unsatisfying.

PRINCIPAL COMPARISON LAB CELL VERSUS MULTILAYER-POUCH CELL

Most lab-scale experiments on (Li-S) batteries use coin-type cells with about 1–6 mAh capacity. Cells being applied in consumer electronics, power tools, drones, and electric vehicles may differ in shape and size but all employ double-sided electrodes and achieve about 0.45–1.2 Ah capacity. Intuitively, this translates into a significant scaling factor (>500) for all cell components when transferring results from lab scale to prototype level. Among the different cell formats (cylindrical, prismatic-hardcase, and pouch), pouch cells seem to be superior for maximizing the specific energy because of the low weight of cell packaging. For manufacturing single prototype cells, stacking of electrodes and separators can be carried out with less effort than winding an electrode-separator stack for cylindrical cells.[24] Also, cell volume changes can be evaluated and eventually better controlled or compensated.[26,39,40] In addition, several stages are feasible, starting from one-layered[32,34] versions with manageable active material amounts and going up to a few[30,31,39,41] and multilayered pouch cells.[21,22,28,39] The higher the stack, the more electrode area and consequently more sulfur-carbon composite is required. A high uniformity of the double-sided coating is needed, which is challenging as sulfur sublimes when state-of-the-art solvents for battery coating inks evaporate. Table 1 and Figure 1 compare the major differences between a lab-scale (coin-type) cell and a multilayer prototype cell. Moreover, associated challenges for different parameters regarding the transfer of research findings from coin to pouch cell are described.

Formats are critical in terms of internal resistance, transferring the electrons from the welded tabs to the opposite side of each electrode in a pouch cell. Also, generating heat is an issue that needs to be precisely considered when enlarging cells. In addition, commercially available lithium foils are only available with 100 mm width limiting common formats being established for LIB.

One-layered pouch cells are more easily assembled, though it is challenging to establish a homogeneous adhesion between the separator and both electrodes in the pouch cell. In addition, the dead volume is higher than that in a multilayered pouch cell. The processability of components and materials (e.g., mechanical stability of coatings and weldability of current collectors) is important. In a coin cell comprising an areal pressure, mechanical disintegration of materials and the accompanied overpotential can be better compensated than in a pouch cell. In pouch cells, however, the pressure distribution on active materials[44] that undergo a volume change can be adapted by applying external pressure.[40] Consequently, one important challenge is to find a rational balancing of cathode loading, electrolyte amount, and anode thickness for optimal energy densities and cycle stability on the cell level.

In conclusion, most lab-scale experiments in Li-S literature do not allow a direct transfer to the practical pouch cell level, and as a consequence, important aspects of the relevant Li-S cell chemistry are overlooked.

Multilayer-pouch cells require several additional process steps and thus add complexity to the system. On the other hand, the reduction of dead volume, better

Table 1. Comparison of Coin Cells with Pouch Cells Regarding the Most Relevant Parameters and Associated Challenges

Parameter	Coin Cell	Multilayered Pouch Cell	Challenges
Material amount required	for cathode testing, 20–100 mg of porous carbon is required for app. 10 × 10 cm^2	depending on the way of coating (one or double sided) and coating process (ink versus dry film): 10–100 g of material >>100 cm^2	scalable synthesis of innovative materials
			pre-milling of particles may influence carbon porosity[42]
Electrode layout	one-sided coating required, spherical shape of electrodes depending on the respective cell (EL, HOHSEN, Swagelok, coin cell)	double-sided coating	development of coating and drying processes that guarantee symmetric coatings on both sides of the foil (thickness, density)
			avoiding sublimation of sulfur on one side when drying the second one
Electrode ink in manufacturing process	various blending techniques possible, swing mills with shearing forces are often employed	pre-mixing or grinding necessary, blending with binders in >500 mL scale necessary	stable, homogeneous suspensions of binder, active material, and conductive additive in larger batches
			applying shearing forces in a larger 500 mL batch is more challenging or needs extra kneading equipment than in a 50 mL swing mill beaker
Electrode coating process	table coater (max. 200 × 300 mm^2 sheet)	slot die or comma bar coating	slot die coating requires homogeneous gas-free ink transportation and avoiding clogging of the slot die equipment
			for comma bar coating, sedimentation of particles can occur during the period of coating leading to inhomogeneous active material loadings
Potential drop and electric resistance	only intrinsic electrode layer resistance, the electric contact works via the entire cathode area	sheet resistance depends on current collector, electrode layer, and tap welding resistance	transfer of innovative material/current collector concepts (e. g., based on carbon) into pouch cells due to the increased ohmic loss along the electrode
			welding metal taps on a carbon current collector
Electrolyte excess required	at least 4–5 µL/mg electrolyte amount per sulfur mass depending on the vapor pressure of the respective solvent	<3 µL/mg electrolyte to sulfur ration; excess is lower compared to coin cell as dead volume is lower to achieve relevant specific energies	minimization of the volume outside of the cell stack ("dead volume") because it needs to be filled with electrolyte, both in coin and in pouch cells
			dead volume minimization in thin CR2016 coin cells is limited to a certain degree to 25 µL by employing increased spacer thickness and leaving out springs
			in pouch cells, dead volume can be decreased by increasing the electrode stack or rather the number of electrodes
Lithium excess	250 µm lithium thickness in combination with 2.2 mg/cm^2 sulfur loading and 70% sulfur utilization results in 20:1 n/p and 19-fold lithium excess	50 µm lithium thickness in combination with 2.2 mg/cm^2 sulfur loading and 70% sulfur utilization results in 4:1 n/p and 3-fold lithium excess	masking of electrolyte depletion and increased cycle life when employing electrolyte excess in combination with lithium excess
			lithium excess drastically lowers the energy density of the corresponding pouch cells
Volume in cell outside of the cell stack (dead volume)	high (app. 25 µL for CR 2016 with 1 mm spacer and 100 µm C/S film on 15 µm Al[43])	app. One magnitude lower than for the described CR2016 set-up depending on stack layout and quantity of electrodes	diffusion of dissolved polysulfides (=active material) in the cell volume outside of the cell stack leading to low Coulombic efficiencies and active material loss that cannot be utilized anymore
Electrolyte filling	by adding droplets via a pipette on one-layered electrode	the entire stack requires electrolyte wetting and soaking, specially adapted filling procedure, vacuum might be applied	achieve homogeneous electrolyte wetting in the entire multilayered electrode cell stack
Pressure	without springs: volume is fixed and no constant pressure conditions With springs: pressure can be slightly adjusted, but dead volume is higher	pouch cell is principally able to inflate and to shrink allowing constant pressure and pressure monitoring by external tools	balancing the volume change of the cathode active material during (de)lithiation, the plating or stripping of lithium, and the electrolyte volume being soaked in or out of the cathode porosity, especially in multilayered pouch cells
Role of porosity of electrodes	cathodes can swell due to electrolyte up-take depending on the spacer and coin cell type, calendared dry electrode density might not be the same after electrolyte soaking or during cycling	porosity and swelling behavior is a key parameter during the (de-) lithiation process when electrolyte is soaked in and out	See "pressure."

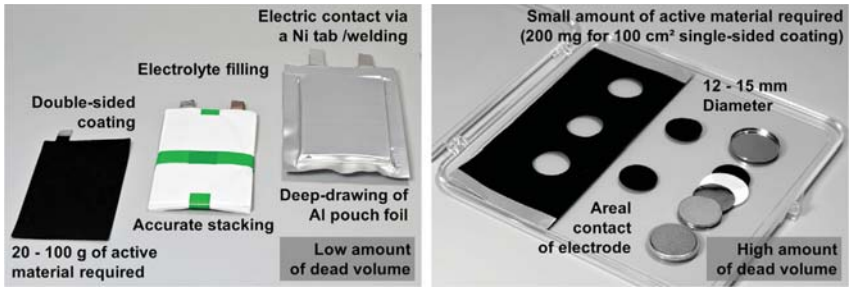

Figure 1. Photographs of a Coin and a Pouch Cell and Their Main Differences According to the Authors' Experience

control of electrolyte content, and external pressure provide significant advantages for reproducible performance evaluation. Vice versa, the worse control on the mentioned parameters is the main disadvantage of coin cell testing and limits the deduction of application-relevant data.

CALCULATIONS OF THE ENERGY (VOLUMETRIC AND GRAVIMETRIC)

As already mentioned in the introduction and by Betz et al.,[45] a transparent calculation of energy density on cell level is crucial. Herein, we calculate both gravimetric and volumetric energy for a multilayered pouch cell (further specifications see Table 2). The calculation of the gravimetric energy density is based on all active and inactive pouch cell components, including the packaging, current collectors, and separator. Volumetric energy density is calculated for the cell stack (cathodes, anodes, electrolyte, and separator) only, cell packaging has not been considered.

The specific energy (in Wh/kg) is calculated by the following equation:

$$E_{Sp} = E_{nom}/m_{cell}, \quad \text{(Equation 1)}$$

Where E_{nom} is the measured value of nominal discharge energy (in Wh) and m_{cell} is the total weight of the cell (in kg) including all its components.

Further, E_{nom} and C_{nom} (in Ah) are calculated by the following equation:

$$E_{nom} = \int U \cdot I\, dt \text{ and } C_{nom} = \int I\, dt. \quad \text{(Equation 2)}$$

The nominal voltage of a cell U_{nom} (in V) is then calculated by dividing the nominal energy by nominal capacity.

$$U_{nom} = E_{nom}/C_{nom}, \quad \text{(Equation 3)}$$

which results in an equation where the specific energy of the cell is a function of nominal capacity, nominal voltage, and total weight of the cell.

$$E_{SP} = C_{nom} \cdot U_{nom}/m_{cell} \quad \text{(Equation 4)}$$

The weight of the cell is calculated by summarizing the weight of all components (in kg), following

$$m_{cell} = m_{Li} + m_{cc-anode} + m_{cathode} + m_{cc-cathode} + m_{sep} + m_E + m_{t+h}, \quad \text{(Equation 5)}$$

with the respective components being indicated by the following indices: lithium-metal anode (Li), anode current collector (cc-anode), all components of the cathode; sulfur, carbon, and binder (cathode), cathode current collector (cc-cathode), separator (sep), electrolyte (E), and tabs and housing (t+h).

Table 2. Definition of the Most Relevant Parameters for the Calculations of Specific Energy and Energy Density

Symbol	Value	Unit	Description
$C_{SP,nom}$	1,313	mAh/g-S	specific capacity related to total mass of sulfur, first discharge with 0.05C
U_{nom}	2.133	V	nominal voltage of first discharge with 0.05C
$n_{cathode}$	15	–	number of double-sided coated cathode
$A_{1,cathode}$	32.66	cm^2	area of 1 cathode coating
$A_{cc,cathode}$	33.3	cm^2	area of 1 cathode current collector (71 × 46 mm^2)
d_{Al}	12	µm	thickness of aluminum foil used as cathode current collector
ρ_{Al}	2.7	g/cm^3	density of aluminum (Gelon)
L_S	1.692	–	sulfur loading (Sigma Aldrich)
ω_S	0.60	–	sulfur content
ω_C	0.25	–	carbon content (Printex XE2-B)
ω_B	0.05	–	binder content: carboxymethyl cellulose cmc (MTI) and styrene-butadiene-rubber SBR (Targray)
ω_{CNT}	0.10	–	CNT content
ρ_S	2.0	g/cm^3	sulfur density
ρ_C	2.2	g/cm^3	carbon density
ρ_B	1.5	g/cm^3	binder density
ρ_{CNT}	2.2	g/cm^3	CNT density (Nanocyl 7000)
$n_{cc,anode}$	16	–	number of anode current collectors (14 100 µm and 2 50 µm)
$A_{cc,anode}$	1.4	cm^2	area of 1 anode current collector flag (copper)
d_{Cu}	10	µm	thickness of copper foil used as anode current collector flag
ρ_{Cu}	8.96	g/cm^3	density of copper (Schlenk)
ρ_{Li}	0.534	g/cm^3	density of lithium (China Energy)
$C_{SP,Li}$	3,860	mAh/g	specific capacity of lithium
N_{exc}	3.645	–	lithium excess (x-fold),
$r_{E/S}$	4.4	µL/mg-S	electrolyte/sulfur ratio
ρ_E	1.2	g/cm^3	electrolyte density 1M LiTFSI + 0.5M $LiNO_3$ in DME/DOL (v:v = 1:1 [Gotion])
A_{sep}	37.5	cm^2	area of 1 sheet of separator (PE)
L_{sep}	0.8	mg/cm^2	areal density of separator material
ϵ_{sep}	0.4	–	porosity of separator
d_{sep}	12	µm	thickness of separator material
$m_{packaging}$	2,470	mg	weight of the packaging plus pouch foil (Shova Denko)
$m_{tab,anode}$	221.9	mg	weight of the anode tab
$m_{tab,cathode}$	76.44	mg	weight of the cathode tab
A_{stack}	37.5	cm^2	area of the cell stack

The weight of elemental Li from the anode is calculated by

$$m_{Li} = (N_{exc} + 1) \cdot L_S \cdot C_{SP,nom} \cdot \frac{A_{anode}}{C_{SP,Li}}, \qquad \text{(Equation 6)}$$

where N_{exc} is a number that describes the total lithium excess in the cell, L_S is the sulfur loading of the cathode (in mg-S/cm^2), $C_{SP,nom}$ is the nominal specific capacity of

the cathode (in mAh/g-S, maximum 1,672 mAh/g-S), A_{anode} is the total electrode geometrical area of the anode (in cm^2, equal to $A_{cathode}$), and $C_{SP,Li}$ is the specific capacity of lithium (in mAh/g-Li, 3,860 mAh/g-Li), see Table 2.

The weight of the anode current collector is described by

$$m_{cc-anode} = A_{cc-anode} \cdot n_{cc-anode} \cdot d_{Cu} \cdot \rho_{Cu}, \quad \text{(Equation 7)}$$

where $A_{cc\text{-}anode}$ is the area of the current collector of a single anode, $n_{CC\text{-}anode}$ is the total number of anodes in the cell, d_{Cu} is the thickness of the copper foil (in μm) that is used as a current collector in the anode, and ρ_{Cu} is the density of copper (in g-Cu/cm^3).

The weight of the cathode is calculated by

$$m_{cathode} = A_{cathode} \cdot L_s / \omega_S, \quad \text{(Equation 8)}$$

where $A_{cathode}$ is the total electrode area of the cathode and ω_S is the mass content of sulfur in the cathode.

The total area of the cathode is described by

$$A_{cathode} = 2 \cdot A_{1,cathode} \cdot n_{cathode}, \quad \text{(Equation 9)}$$

where $A_{1,eletrode}$ is the area of 1 cathode electrode and $n_{cathode}$ is the number of double-sided coated cathodes in the cell.

The weight of the cathode current collector is calculated according to the following equation

$$m_{cc-cathode} = A_{cc-cathode} \cdot n_{cathode} \cdot d_{Al} \cdot \rho_{Al}, \quad \text{(Equation 10)}$$

where $A_{cc\text{-}cathode}$ is the number of cathode current collectors, d_{Al} is the thickness of the aluminum foil (in μm), and ρ_{Al} is the density of aluminum (in g/cm^3).

Each side of the double-sided coated cathode is separated from the anode by 1 sheet of separator; the weight of the separator is described by

$$m_{sep} = A_{sep} \cdot 2 \cdot n_{cathode} \cdot L_{sep}, \quad \text{(Equation 11)}$$

where A_{sep} is the area of 1 sheet of separator (in cm^2) and L_{sep} is the areal density of the separator.

The weight of the electrolyte is calculated by

$$m_E = A_{cathode} \cdot L_S \cdot r_{E/S} \cdot \rho_E, \quad \text{(Equation 12)}$$

where $r_{E/S}$ is the ratio of the volume of the electrolyte and the total mass of sulfur in the cell (in μL-E/mg-S) and ρ_E is the density of the liquid electrolyte.

The additional weight of the tabs and housing plus packaging is a constant and depends on the materials used and the format of the cell. The calculations presented in this perspective were carried out using the values for tabs and housing plus packaging from Table 2.

The volumetric energy density (in Wh/L) is calculated by

$$E_{vol} = C_{nom} \cdot V_{nom} / V_{cell}, \quad \text{(Equation 13)}$$

where V_{nom} is the volume of the cell (excluding t+h), described by the following equation

$$V_{cell} = \left(d_{Li,all} + d_{Al,all} + d_{Sep,all}\right) \cdot A_{stack} + V_{cathode}, \quad \text{(Equation 14)}$$

where $d_{Li,all}$ is the total thickness of all lithium in the cell (in μm), $d_{Al,all}$ is the total thickness of the current collector in the cell (in μm), $d_{Sep,all}$ is the thickness of all separator sheets in the cell, A_{stack} is the area of the cell stack (in cm^2, see Table 2), and $V_{cathode}$ is the volume of the cathode (in cm^3) including all components of the cathode and a certain porosity filled with liquid electrolyte.

The thickness of all lithium is calculated by the following equation

$$d_{Li,all} = (N_{exc} + 1) \cdot L_S \cdot C_{SP,nom} \cdot A_{cathode} \cdot n_{anode} / (C_{SP,Li} \cdot \rho_{Li} \cdot A_{anode}), \quad \text{(Equation 15)}$$

where ρ_{Li} is the density of lithium.

The thickness of all cathode current collectors is calculated by

$$d_{Al,all} = d_{Al} \cdot n_{cathode}. \quad \text{(Equation 16)}$$

The thickness of all separators is calculated by

$$d_{Sep,all} = d_{sep} \cdot n_{cathode}, \quad \text{(Equation 17)}$$

where d_{sep} is the thickness of the separator.

The volume of cathode $V_{cathode}$ is the sum of the total volume of the solid components and the porous and with electrolyte filled volume of the cathode coating $V_{cathode,poro}$.

$$V_{cathode} = V_{cathode,\ comp} + V_{cathode,\ poro}, \quad \text{(Equation 18)}$$

where $V_{cathode,comp}$ is the volume of the compact cathode raw materials (in cm^3, for mass fractions see Table 2), it stands for all solid components of cathode, S [sulfur], C [carbon], B [binder], and CNT [carbon nanotubes]. m_i is the weight of the individual component [see below] and ρ_i its density (see Table 2)

$$V_{cathode,comp} = \sum_i \frac{m_i}{\rho_i} = \frac{m_S}{\rho_S} + \frac{m_C}{\rho_C} + \frac{m_B}{\rho_B} + \frac{m_{CNT}}{\rho_{CNT}}. \quad \text{(Equation 19)}$$

The weight of total sulfur in the cell is calculated by

$$m_S = A_{cathode} \cdot L_s. \quad \text{(Equation 20)}$$

The weight of total carbon in the cell is calculated by

$$m_C = m_{cathode} \cdot \omega_C, \quad \text{(Equation 21)}$$

where ω_C is the mass fraction of carbon in the cell.

The weight of the binder is calculated by

$$m_B = m_{cathode} \cdot \omega_B, \quad \text{(Equation 22)}$$

where ω_B is the mass fraction of binder in the cell.

Total weight of CNT is calculated by

$$m_{CNT} = m_{cathode} \cdot \omega_{CNT}, \quad \text{(Equation 23)}$$

where ω_{CNT} is the mass fraction of CNT in the cell.

The volume of the porous part of the cathode is described by the following equation, including the liquid electrolyte and taking in to account that a part of the electrolyte fills the porosity of the separator.

$$V_{cathode,poro} = V_E - V_{sep,\ poro}, \quad \text{(Equation 24)}$$

where V_E is the total volume of electrolyte in the cell (in cm^3) and $V_{sep,poro}$ is the porous volume of the separator filled with liquid electrolyte.

Total volume of the electrolyte is calculated by

$$V_E = A_{cathode} \cdot L_S \cdot r_{E/S} \quad \text{(Equation 25)}$$

The volume of the electrolyte in separator porosity is described by

$$V_{sep,poro} = A_{sep} \cdot 2 \cdot n_{cathode} \cdot d_{sep} \cdot \epsilon_{sep}, \quad \text{(Equation 26)}$$

where ϵ_{sep} is the porosity of the separator (provided by the supplier, see Table 2).

Impact of Electrolyte and Anode Excess

Similar to lithium-metal batteries versus an NMC-based cathode,[24] the most significant source for misinterpretations of lab cell results is related to the electrolyte and anode excess masking the major degradation mechanisms in Li-S cells. The electrolyte is involved not only in ionic transport but also strongly influences the cathode conversion chemistry.[5] The cathode reaction mechanism is highly affected by the electrolyte content[46,47] as the dilution factor of polysulfides determines dissolution and precipitation equilibria. Furthermore, the ionic mobility and electrolyte viscosity strongly depends on the polysulfide concentration with impact on the internal cell resistance. Even more importantly, consumption of electrolyte components by the anode surface is known to be the most relevant degradation phenomena. A high excess of electrolyte according to state of the art (SOTA) containing 1,2-dimethoxyethane (DME), 1,3-dioxolane (DOL), Lithium bis(trifluoromethanesulfonyl)imide (LiTFSI), and lithium nitrate ($LiNO_3$) implies an endless $LiNO_3$ reservoir for SEI repair, hence masking anode degradation under real (lean) conditions. Thus, electrolyte volume referenced to the sulfur mass in the cathode (E:S or E:C) has tremendous impact on cycle life, rate capability, and specific cathode utilization, especially at high loadings.[48] In detail, high E:S ratio[49] usually enhances cycle life as electrolyte depletion proceeds over a longer timespan before dry out leads to cell failure. As a consequence of these phenomena, the electrolyte content has implications on other cell components as well.

Often neglected parameters, such as pressure on cell stack,[26,39] porosity,[48] and swelling capability of electrodes as well as separators,[28,50] are expected to all impact the cell performance indirectly through interfering with the electrolyte volume being soaked up in the cell stack.

Within the past two years, the degree of cathode densification and the impact on prospective prototype cell performance has been systematically investigated in DME/DOL ether-based standard electrolyte.[48,51] In those studies, the increasing cathode density results in a significant overpotential in the second plateau region being in good agreement with the author's experience. The overpotential can be attributed to reduced ionic mobility and accompanied by high viscosity[52] due to the limited pore volume for the electrolyte take-up.

Those findings imply that a comparison of components and materials will likely be influenced by electrode porosity and the capability to soak up electrolyte rather than intrinsic carbon porosity. In order to exclude such secondary impact, porosity, pressure, and swelling capability of cell components need to be carefully monitored in comparative studies. Similarly, lithium metal is typically used in huge (15- to 20-

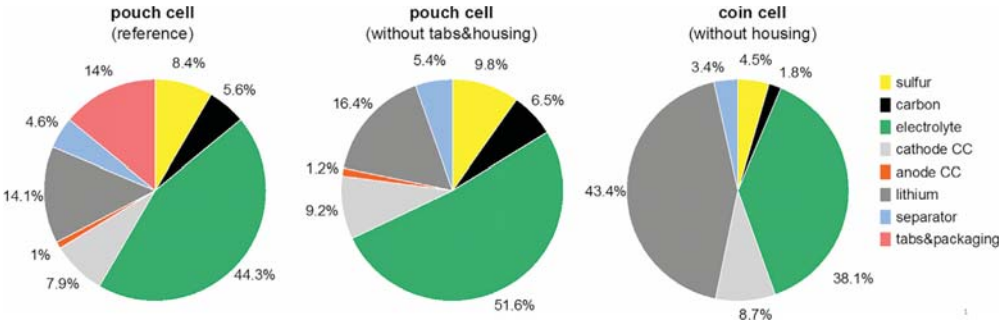

Figure 2. Mass Distribution for Three Scenarios

The components of the reference pouch cell (left), the same pouch cell excluding the weight of the tabs and housing (middle), and a Li-S coin cell excluding coin cell housing (right). The same parameters as for the pouch cell were used to calculate the mass distribution for the coin cell (Table 2). Additional parameters for the coin cell: cathode diameter of 15 mm; diameter of Li chip, 16.5 mm; thickness of Li chip, 250 μm; electrolyte/sulfur ratio, 7 μL/mg S; and diameter of separator, 19 mm.

fold) excess,[24] usually leading to a higher ratio of anode and cathode loading (N/P ratio). Besides electrolyte decomposition, lithium-metal consumption is one of the major degradation phenomena through SEI and "dead lithium" formation upon cycling;[22,26] hence, a higher N/P ratio leads to a higher cycle stability.

Re-evaluating Factors for Energy Density Improvement

One critical parameter is the estimation of energy density on prototype cell level. Very often, this parameter is calculated by multiplying the capacity with the average voltage being measured in half-cells versus lithium. 2,660 Wh/kg is the theoretical energy density of a Li-S cell. Theoretical estimations by Betz et al.[45] for a cylindrical 18,650-cell geometry show that the final specific energy density including all components and housing is as low as 277 Wh/kg. However, cylindrical cells are not the optimal geometry in order to bring out the beneficial features of a Li-S cell as the housing is comparatively heavy. According to Lu et al.,[48] pouch cells are basically the type of cell offering the best ratio of active to inactive material mass.

Naturally, providing an excess of electrolyte and lithium in order to enhance the cycle life of cells has obvious limitations when considering the cell's energy density. Even at moderate lithium and electrolyte excess, both components take a significant fraction of the cell's volume and weight. Similar to NMC-based lithium-metal batteries,[24] conditions in most test cell environments (electrolyte to sulfur ratio; volume per mass or mass per mass E/S >4 μL/mg sulfur and n/p > 4) translate in specific energy values well below 100 Wh/kg also for Li-S cells. It is reported that electrolyte content takes by far the largest fraction of presently developed prototype cells,[48,53] even at moderate values of E/S = 4 μL/mg sulfur. This finding is in good agreement with the estimations presented in the following. Given that carbon and sulfur have intrinsically low mass densities, the inactive material mass portion is rather high compared to LIBs.

In recent literature, the areal active material loading has been identified as a crucial parameter for increasing energy density, and recent publications report on values exceeding 10 mg/cm^2.[50]

Furthermore, the sulfur/carbon ratio is often considered to be an important factor.[48,50] The motivation of increasing loading levels thereby is to minimize the mass and volume fractions of the inactive cell components. However, the impact

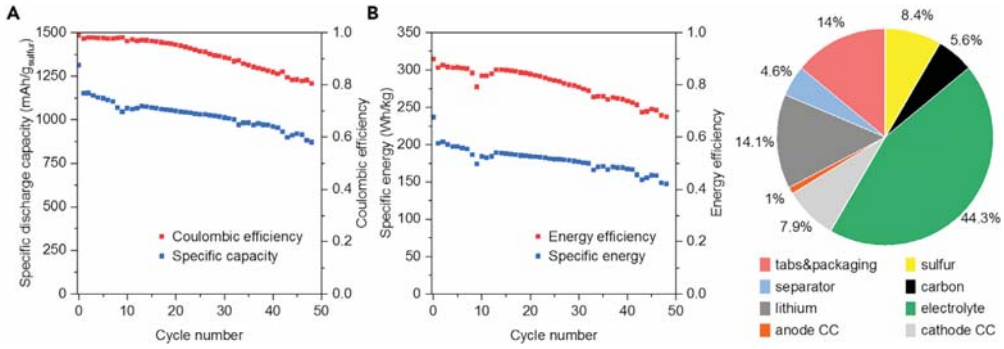

Figure 3. Parameters for the IWS Reference Cell

Specific capacity and Coulombic efficiency over cycle number (A), specific energy and energy efficiency over cycle number (B), and component mass distribution according to the IWS cell design and development (C).

of an Al current collector, separator, and carbon in a typical Li-S cell is rather low as they only take a minor fraction of volume and weight, even at moderate loading levels.[48] It should be noted that mass fractions of components highly depend on the overall cell design. As an example, introducing a 10 μm copper foil as the anode current collector will change the mass fraction of all components significantly. The relations and conclusions discussed here are therefore closely related to the design of our reference cell (Figure 1, 2, 3, and 4; Table 2), which is usually prepared as follows: cathodes used herein consist of a Printex carbon black-sulfur composite and a small fraction of multi-walled carbon nanotubes (MWCNTs) as the conductive additive. A mixture of carboxymethyl cellulose (CMC) and styrene-butadiene-rubber (SBR) as a binder was added. The mixture was adjusted to achieve a sulfur content of 60% in the electrode. The cathode was produced via roll-to-roll processing (Jakob Weiß & Söhne Maschinenfabrik GmbH [JWS]) and a slot die (FMP Technology GmbH). The electrodes were vacuum dried at 50°C for 1 h prior to cell assembly. For the latter, the cathode was assembled against a Li anode (China Energy) and separated through a polyethylene (PE) separator (12 μm). Pouch cells (71 × 46 mm^2) were assembled using double-side coated cathodes. Cells were cycled between 1.9 and 2.6 V versus metallic lithium. The current rate for all measurement was C/20 for the formation cycle, and subsequent cycling was conducted with a C/10 rate.

The sensitivity analysis of the reference cell confirms only a minor impact of the sulfur loading level for values above 3 mAh/cm^2 (Figure 4C), while minimizing the electrolyte content is key for both gravimetric and volumetric energy density (Figure 4B). Because of the low mass density of metallic lithium, the anode excess limits the volumetric energy density much more than the specific energy (Figure 4A). Considering the minor impact of high active material loadings on energy density, the recent trend in further maximizing sulfur loadings[49] to 10 mAh/cm^2 and beyond seems to be questionable (Figure 4C).

Furthermore, high active material loadings have several other consequences being often neglected. First of all, the internal resistance will significantly increase, as the ionic transport in the electrolyte is known to be a determining factor.[41,52] Both, similar to NMC-based lithium-metal batteries,[24] the electrode distance as well as the areal current will increase at a given C-rate, when increasing the loading level, with negative implications on the power capability of the system. According to Chen et al., the increase in areal current has another crucial impact being related

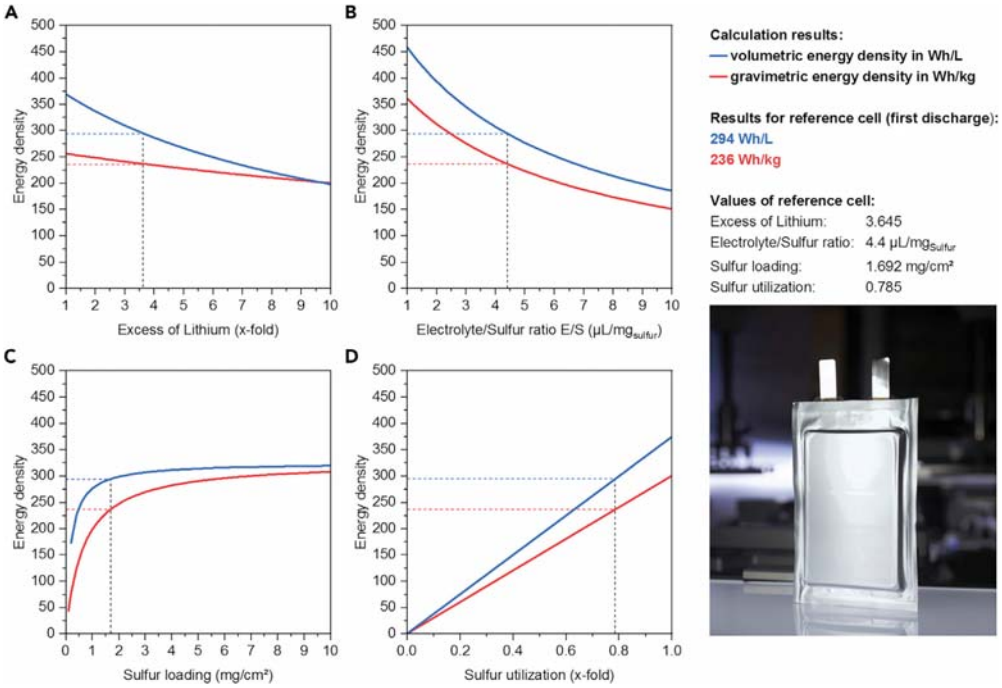

Figure 4. Projected Energy Density (Gravimetric and Volumetric) of the Reference Cell
The amount of Li-excess (A), electrolyte/sulfur E/S ratio (B), sulfur-loading (C), and sulfur utilization (C).

to the major anode degradation phenomena of Li-S cells. Dendritic growth and electrolyte decomposition are known to be dependent on the charging current per area. Thus, under realistic conditions (at low excess of Li and electrolyte), the cell's cycle life will be drastically lowered with increasing active material loadings and a given charging C-rate.[24]

IMPLICATIONS FOR FUTURE INVESTIGATIONS

In order to advance Li-S technology toward a wider applicability, development and testing of cell components need to be performed under realistic conditions. Furthermore, from this holistic viewpoint, new scientific questions arise that need to be addressed by fundamental research regarding both lab cell and prototype cell research. Scientists are committed to reconsider and adapt their cell setups and characterization protocols for establishing fair and comparative evaluation.

Li-S Pouch Cell Development toward Industrialization

The commercial success of Li-S accumulators will depend on its capability to meet the major requirements for specific applications. In order to test and optimize the required performance parameters close-to-application multilayer-pouch cells are most likely the ideal environment. Introducing new materials and concepts require confirmed pouch cell performance under realistic conditions. Data derived from coin-type cell testing typically do not allow for deriving decisive characteristics (energy density, power capability, and safety) being relevant for such application-oriented development. In addition, the effect of pressure application on pouch cells being investigated requires reinvestigation.

Table 3. Recommendations for Reporting Parameters in Lithium-Sulfur-Battery Lab-Scale Testing

Parameter	Recommendation
Cathode parameter	tap density of the cathode in g/cm^3 before and ideally after cycling, thickness and areal loading of sulfur in mg/cm^2, all cathode components (binder, conductive additive etc.) and their characteristics (composition, batch label etc.), current collector (thickness, areal mass)
Coin cell	type should be stated (CR2032, 2016, Swaglok, Hohsen, etc.); applied crimping pressure or spring force or type
Separator	at least: thickness, material (PP, GF, or PE) and ideally: the manufacturer
Lithium anode	chip thickness and diameter, or n/p ratio
Electrolyte	type of electrolyte and amount based on the sulfur mass (E/S ratio)
Operation voltage window	the discharge cut-off voltage should be adjusted to the electrolyte depletion window, especially when using $LiNO_3$ as additive
Temperature	should be stated for each graph

Fundamental Scientific Questions Requiring More Attention and Dedicated Testing Environment

Because of the complex process line and high material amount being required for pouch cell manufacturing, materials and electrolyte screening via pouch cells would be inefficient. Hence, there is still considerable need for lab-scale methods for the pre-evaluation of cell components as well as to study fundamental mechanisms under realistic conditions. To guarantee meaningful screening parameters that are transferable to pouch cell design, the following considerations should be taken into account.

The electrolyte is the most influential component and will most likely take the largest mass fraction even in optimized Li-S cells (Figure 2). It can be assumed that E/S ratios <<4 μL/mg will be required in order to achieve a specific energy exceeding today's Li-ion cells—not only for the Li-S system, but also for metallic lithium as a generic anode. At the same time, the electrolyte content impacts all cell's key performance indicators through its specific interactions with all cell components. As a consequence, a solid understanding of those interactions under restricted electrolyte volume is required in order to improve cell performance.

Ideally, new test cells shall be designed allowing the control and minimization of electrolyte content and constant pressure distribution on the electrode stack.[40] In addition, methods to investigate the swelling behavior of cathodes in various electrolytes *in situ* should be established.

Further investigation of the lithium, electrolyte, and additive consumption per cycle including their solid, liquid, or gaseous decomposition[24] products under various conditions and for different electrolyte systems would be of high value. Understanding ionic mobility within highly concentrated (saturated) polysulfide solutions in various electrolytes would be another important aspect.

Recommendations for Reporting Parameters

Nevertheless, similar to the recommendations given by Cao et al.,[50] the parameters given in Table 3 should be regarded as a mandatory quality standard in scientific reporting by authors, reviewers, and publishing editors and an integration in peer-review processes is highly desirable.

CONCLUSIONS

As already discussed by other perspectives, application-relevant data (such as cycle life, rate capability, and energy density) are inaccessible via electrochemical standard tests in today's Li-S-lab cells because of electrolyte and anode excess masking major degradation mechanisms. Because of the gap of lab cell characterization and prototype cell development, misinterpretations and false expectations are frequently reported: material property impacts are often over-interpreted, while parameters with indirect impact (e.g., electrode and separator porosity and pressure on cell stack) are neglected.

In order to improve the relevance and scientific progress in Li-S-technology, rapid transfer and evaluation of new concepts on prototype (multilayer-pouch) cell level is essential, especially for electrolytes working in a lean electrolyte regime. Furthermore, fundamental studies should concentrate on fundamental scientific questions related to the main bottlenecks of Li-S-cells: understanding anode and electrolyte degradation phenomena and realistic evaluation of stabilizing interfaces (e.g., via protective coatings and electrolyte additives in a lean electrolyte regime). For such advances, new analytical tools allowing electrochemical studies under lean electrolyte conditions and *in situ* studies of electrolyte and additive depletion pose tremendous chances for impactful research. In addition, tap density and the accompanied swelling and compaction behavior of cathodes in different electrolytes should be further addressed. Consequently, pressure distribution in pouch cells should be monitored and adapted to the respective mechanical properties of the cathode and anode, respectively. With these guidelines and continued efforts, Li-S technology will further improve fostering its breakthrough as a sustainable, safe, and lightweight energy storage option in the near future.

ACKNOWLEDGMENTS

This work has received funding from the Federal Ministry of Education and Research (BMBF); support codes 03XP0030B (StickLiS), 03XP0031A (SepaLiS), 03XP0133D (LiBEST), 03XP0178A (HiPoLiS), and 03XP0185A (MaLiBa); from the European Union's Horizon 2020 research and innovation program under grant agreement No. 666157 (ALISE) and No. 814471 (LISA); and Eurostars support code 01QE1837B (LiMeCut).

AUTHOR CONTRIBUTIONS

S.D. and H.A. wrote the paper and contributed equally. P.H. carried out the calculations on prototype cell level and detailed sensitivity analysis. T.A. contributed to the calculations and provided valuable discussions on cell manufacturing, cell swelling, and testing. B.S. provided valuable discussion on electrode processability and swelling behavior. S.K. supervised the entire work and contributed especially to the Introduction and Conclusion.

REFERENCES

1. Rauh, R.D. (1979). A lithium/dissolved sulfur battery with an organic electrolyte. J. Electrochem. Soc. *126*, 523.

2. Rauh, R.D., Shuker, F.S., Marston, J.M., and Brummer, S.B. (1977). Formation of lithium polysulfides in aprotic media. J. Inorg. Nucl. Chem. *39*, 1761–1766.

3. Yamin, H. (1988). Lithium sulfur battery. J. Electrochem. Soc. *135*, 1045.

4. Chu, M.-Y., De Jonghe, L.C., Visco, S.J., and Katz, B.D. Liquid electrolyte lithium-sulfur batteries US patent US00603072OA, filed Oct. 10, 1997 and granted Feb. 29, 2000.

5. Wild, M., O'Neill, L., Zhang, T., Purkayastha, R., Minton, G., Marinescu, M., and Offer, G.J. (2015). Lithium sulfur batteries, a mechanistic review. Energy Environ. Sci. *8*, 3477–3494.

6. Peng, H.-J., Huang, J.-Q., Cheng, X.-B., and Zhang, Q. (2017). Review on high-loading and high-energy lithium-sulfur batteries. Adv. Energy Mater. *7*, 1700260.

7. Peng, H.J., Huang, J.Q., and Zhang, Q. (2017). A review of flexible lithium-sulfur and analogous alkali metal-chalcogen rechargeable batteries. Chem. Soc. Rev. *46*, 5237–5288.

8. Wild, M., and Offer, G. (2019). Lithium Sulfur Batteries (John Wiley & Sons Incorporated).

9. Aurbach, D., Pollak, E., Elazari, R., Salitra, G., Kelley, C.S., and Affinito, J. (2009). On the surface chemical aspects of very high energy density, rechargeable Li–sulfur batteries. J. Electrochem. Soc. *156*, A694.

10. Yan, C., Zhang, X.-Q., Huang, J.-Q., Liu, Q., and Zhang, Q. (2019). Lithium-anode protection in lithium–sulfur batteries. J. Trends Chem. *1*, 693–704.

11. Lerwill, D. (2009). Energy is close to achieving 500Wh/kg and is targeting 600Wh/kg with solid state lithium sulfur technology (OXIS Energy Ltd), January 22, 2020. https://oxisenergy.com/https-oxisenergy-com-wp-content-uploads-2020-01-500-and-600-whkg-pressor-pdf/.

12. Cook, C. (2019). Application-driven cathode design for high energy and high power Li-S batteries. Carbon Electrode Materials. Workshop (Dresden).

13. Ye, Y., Wu, F., Liu, Y., Zhao, T., Qian, J., Xing, Y., Li, W., Huang, J., Li, L., Huang, Q., et al. (2017). Toward practical high-energy batteries: A modular-assembled oval-like carbon microstructure for thick sulfur electrodes. Adv. Mater. *29*, 1700598.

14. Fotouhi, A., Auger, D., O'Neill, L., Cleaver, T., and Walus, S. (2017). Lithium-sulfur battery technology readiness and applications—a review. Energies *10*, 1937.

15. Cleaver, T., Kovacik, P., Marinescu, M., Zhang, T., and Offer, G. (2018). Perspective—commercializing lithium sulfur batteries: are we doing the right research? J. Electrochem. Soc. *165*, A6029–A6033.

16. Wang, W., Yue, X., Meng, J., Wang, J., Wang, X., Chen, H., Shi, D., Fu, J., Zhou, Y., Chen, J., and Fu, Z. (2019). Lithium phosphorus oxynitride as an efficient protective layer on lithium metal anodes for advanced lithium-sulfur batteries. Energy Storage Mater. *18*, 414–422.

17. Pang, Q., Liang, X., Shyamsunder, A., and Nazar, L.F. (2017). An in vivo formed solid electrolyte surface layer enables stable plating of Li metal. Joule *1*, 871–886.

18. Cheng, X.-B., Yan, C., Chen, X., Guan, C., Huang, J.-Q., Peng, H.-J., Zhang, R., Yang, S.-T., and Zhang, Q. (2017). Implantable solid electrolyte interphase in lithium-metal batteries. Chem *2*, 258–270.

19. Zhang, R., Chen, X., Shen, X., Zhang, X.-Q., Chen, X.-R., Cheng, X.-B., Yan, C., Zhao, C.-Z., and Zhang, Q. (2018). Coralloid carbon fiber-based composite lithium anode for robust lithium metal batteries. Joule *2*, 764–777.

20. Zhang, H., Oteo, U., Judez, X., Eshetu, G.G., Martinez-Ibañez, M., Carrasco, J., Li, C., and Armand, M. (2019). Designer anion enabling solid-state lithium-sulfur batteries. Joule *3*, 1689–1702.

21. Weller, C., Thieme, S., Härtel, P., Althues, H., and Kaskel, S. (2017). Intrinsic shuttle suppression in lithium-sulfur batteries for pouch cell application. J. Electrochem. Soc. *164*, A3766–A3771.

22. Cheng, X.-B., Yan, C., Huang, J.-Q., Li, P., Zhu, L., Zhao, L., Zhang, Y., Zhu, W., Yang, S.-T., and Zhang, Q. (2017). The gap between long lifespan Li-S coin and pouch cells: the importance of lithium metal anode protection. Energy Storage Mater. *6*, 18–25.

23. Borchardt, L., Oschatz, M., and Kaskel, S. (2016). Carbon materials for lithium sulfur batteries-ten critical questions. Chemistry *22*, 7324–7351.

24. Chen, S., Niu, C., Lee, H., Li, Q., Yu, L., Xu, W., Zhang, J.-G., Dufek, E.J., Whittingham, M.S., Meng, S., et al. (2019). Critical parameters for evaluating coin cells and pouch cells of rechargeable Li-metal batteries. Joule *3*, 1094–1105.

25. Liu, J., Bao, Z., Cui, Y., Dufek, E.J., Goodenough, J.B., Khalifah, P., Li, Q., Liaw, B.Y., Liu, P., Manthiram, A., et al. (2019). Pathways for practical high-energy long-cycling lithium metal batteries. Nat. Energy *4*, 180–186.

26. Niu, C., Lee, H., Chen, S., Li, Q., Du, J., Xu, W., Zhang, J.-G., Whittingham, M.S., Xiao, J., and Liu, J. (2019). High-energy lithium metal pouch cells with limited anode swelling and long stable cycles. Nat. Energy *4*, 551–559.

27. Weber, R., Genovese, M., Louli, A.J., Hames, S., Martin, C., Hill, I.G., and Dahn, J.R. (2019). Long cycle life and dendrite-free lithium morphology in anode-free lithium pouch cells enabled by a dual-salt liquid electrolyte. Nat. Energy *4*, 683–689.

28. Salihoglu, O., and Demir-Cakan, R. (2017). Factors affecting the proper functioning of a 3Ah Li-S pouch cell. J. Electrochem. Soc. *164*, A2948–A2955.

29. Huang, J.-Q., Zhai, P.-Y., Peng, H.-J., Zhu, W.-C., and Zhang, Q. (2017). Metal/nanocarbon layer current collectors enhanced energy efficiency in lithium-sulfur batteries. Sci. Bull. *62*, 1267–1274.

30. Dai, F., Shen, J., Dailly, A., Balogh, M.P., Lu, P., Yang, L., Xiao, J., Liu, J., and Cai, M. (2018). Hierarchical electrode architectures for high energy lithium-chalcogen rechargeable batteries. Nano Energy *51*, 668–679.

31. Jia, L., Wang, J., Chen, Z., Su, Y., Zhao, W., Wang, D., Wei, Y., Jiang, K., Wang, J., Wu, Y., et al. (2019). High areal capacity flexible sulfur cathode based on multi-functionalized super-aligned carbon nanotubes. Nano Res. *12*, 1105–1113.

32. Li, X., Banis, M., Lushington, A., Yang, X., Sun, Q., Zhao, Y., Liu, C., Li, Q., Wang, B., Xiao, W., et al. (2018). A high-energy sulfur cathode in carbonate electrolyte by eliminating polysulfides via solid-phase lithium-sulfur transformation. Nat. Commun. *9*, 4509.

33. Zhang, J., You, C., Wang, J., Xu, H., Zhu, C., Guo, S., Zhang, W., Yang, R., and Xu, Y. (2019). Confinement of sulfur species into heteroatom-doped, porous carbon container for high areal capacity cathode. Chem. Eng. J. *368*, 340–349.

34. Fan, Z., Ding, B., Guo, H., Shi, M., Zhang, Y., Dong, S., Zhang, T., Dou, H., and Zhang, X. (2019). Dual dopamine derived polydopamine coated N-doped porous carbon spheres as a sulfur host for high-performance lithium-sulfur batteries. Chemistry *25*, 10710–10717.

35. Lochala, J., Liu, D., Wu, B., Robinson, C., and Xiao, J. (2017). Research progress toward the practical applications of lithium-sulfur batteries. ACS Appl. Mater. Interfaces *9*, 24407–24421.

36. Qu, C., Chen, Y., Yang, X., Zhang, H., Li, X., and Zhang, H. (2017). LiNO3-free electrolyte for Li-S battery: a solvent of choice with low Ksp of polysulfide and low dendrite of lithium. Nano Energy *39*, 262–272.

37. Kong, L., Jin, Q., Huang, J.-Q., Zhao, L.-D., Li, P., Li, B.-Q., Peng, H.-;J., Zhang, X., and Zhang, Q. (2019). Nonuniform redistribution of sulfur and lithium upon cycling: probing the origin of capacity fading in lithium–sulfur pouch cells. Energy Technol. *7*, 1900111.

38. Lee, C.W., Pang, Q., Ha, S., Cheng, L., Han, S.D., Zavadil, K.R., Gallagher, K.G., Nazar, L.F., and Balasubramanian, M. (2017). Directing the lithium-sulfur reaction pathway via sparingly solvating electrolytes for high energy density batteries. ACS Cent. Sci. *3*, 605–613.

39. Waluś, S., Offer, G., Hunt, I., Patel, Y., Stockley, T., Williams, J., and Purkayastha, R. (2018). Volumetric expansion of lithium-sulfur cell during operation – fundamental insight into applicable characteristics. Energy Storage Mater. *10*, 233–245.

40. Müller, V., Scurtu, R.-G., Richter, K., Waldmann, T., Memm, M., Danzer, M.A., and Wohlfahrt-Mehrens, M. (2019). Effects of mechanical compression on the aging and the expansion behavior of si/C-composite|NMC811 in different lithium-ion battery cell formats. J. Electrochem. Soc. *166*, A3796–A3805.

41. Chung, S.H., and Manthiram, A. (2018). Designing lithium-sulfur batteries with high-loading cathodes at a lean electrolyte condition. ACS Appl. Mater. Interfaces *10*, 43749–43759.

42. Kensy, C., Härtel, P., Maschita, J., Dörfler, S., Schumm, B., Abendroth, T., Althues, H., Lotsch, B.V., and Kaskel, S. (2020). Scalable production of nitrogen-doped carbons for multilayer lithium-sulfur battery cells. Carbon *161*, 190–197.

43. Dörfler, S., Strubel, P., Jaumann, T., Troschke, E., Hippauf, F., Kensy, C., Schökel, A., Althues, H., Giebeler, L., Oswald, S., and Kaskel, S. (2018). On the mechanistic role of nitrogen-doped carbon cathodes in lithium-sulfur batteries with low electrolyte weight portion. Nano Energy *54*, 116–128.

44. Maiga, O.I.A., Li, R., Ye, K.F., Liu, B.H., and Li, Z.P. (2019). Sulfide heave: key factor governing cathode deterioration in pouch Li S cells. Electrochim. Acta *300*, 150–155.

45. Betz, J., Bieker, G., Meister, P., Placke, T., Winter, M., and Schmuch, R. (2019). Theoretical versus practical energy: a plea for more transparency in the energy calculation of different rechargeable battery systems. Adv. Energy Mater. *9*, 1803170.

46. Brückner, J., Thieme, S., Grossmann, H.T., Dörfler, S., Althues, H., and Kaskel, S. (2014). Lithium–sulfur batteries: influence of C-rate, amount of electrolyte and sulfur loading on

cycle performance. J. Power Sources *268*, 82–87.

47. Emerce, N.B., and Eroglu, D. (2019). Effect of electrolyte-to-sulfur ratio in the cell on the Li-S battery performance. J. Electrochem. Soc. *166*, A1490–A1500.

48. Lu, D., Li, Q., Liu, J., Zheng, J., Wang, Y., Ferrara, S., Xiao, J., Zhang, J.G., and Liu, J. (2018). Enabling high-energy-density cathode for lithium-sulfur batteries. ACS Appl. Mater. Interfaces *10*, 23094–23102.

49. Bhargav, A., He, J., Gupta, A., and Manthiram, A. (2020). Lithium-sulfur batteries: attaining the critical metrics. Joule *4*, 285–291.

50. Cao, Y., Li, M., Lu, J., Liu, J., and Amine, K. (2019). Bridging the academic and industrial metrics for next-generation practical batteries. Nat. Nanotechnol. *14*, 200–207.

51. Kang, N., Lin, Y., Yang, L., Lu, D., Xiao, J., Qi, Y., and Cai, M. (2019). Cathode porosity is a missing key parameter to optimize lithium-sulfur battery energy density. Nat. Commun. *10*, 4597.

52. Vijayakumar, M., Govind, N., Walter, E., Burton, S.D., Shukla, A., Devaraj, A., Xiao, J., Liu, J., Wang, C., Karim, A., and Thevuthasan, S. (2014). Molecular Structure and stability of dissolved lithium polysulfide species. Phys. Chem. Chem. Phys. *16*, 10923–10932.

53. Rikarte, J. (2019). Lithium electrodes for high performance Li-S batteries Lithium-Metal Anodes. Workshop (Dresden).